Hydroxygenkwanin suppresses proliferation, invasion and migration of osteosarcoma cells via the miR-320a/SOX9 axis

XINLI DONG[1], YANHUA WANG[2], HUA ZHUANG[1] and GANG AN[3]

Departments of [1]Orthopedics and [2]Nursing, Traditional Chinese Medicine Hospital of Binzhou, Binzhou, Shandong 256600;
[3]Department of Orthopedics, The First Affiliated Hospital of Harbin Medical University,
Harbin, Heilongjiang 150000, P.R. China

Abstract. Hydroxygenkwanin (HGK) has an anticancer effect in a variety of tumors, but its role in osteosarcoma has not been explored. The purpose of the present study was to investigate the therapeutic effect of HGK on osteosarcoma and its specific molecular mechanism. Osteosarcoma cells (MG-63 and U2OS) treated with various concentrations of HGK were assigned to the treatment group. MTT, clone formation, wound healing and Transwell assays were performed to assess the viability, proliferation, migration, and invasion of MG-63 and U2OS cells. RT-qPCR was conducted to quantify the expression levels of of microRNA (miR)-320a and SRY-box transcription factor 9 (SOX9) in MG-63 and U2OS cells. The binding sites of miR-320a and SOX9 were predicted by star-Base database, and verified using the dual-luciferase reporter assay. The expression levels of SOX9 and EMT-related proteins (N-cadherin, E-cadherin and vimentin) were detected by western blot analysis. HGK inhibited cell proliferation, migration, invasion, but promoted the expression of miR-320a in MG-63 and U2OS cells. Downregulation of miR-320a reversed the effects of HGK on proliferation, migration and invasion of MG-63 and U2OS cells, while upregulation of miR-320a had the opposite effect. HGK inhibited the expression of SOX9 by promoting the expression of miR-320a. Upregulation of SOX9 could partially reverse miR-320a-induced migration and invasion of MG-63 and U2OS cells. In addition, upregulation of miR-320a promoted E-cadherin expression and inhibited the expression of N-cadherin and vimentin, and the effect of miR-320a was also reversed by SOX9. In conclusion, HGK inhibited proliferation, migration and invasion of MG-63 and U2OS cells through the miR-320a/SOX9 axis.

Correspondence to: Dr Gang An, Department of Orthopedics, The First Affiliated Hospital of Harbin Medical University, 23 Post Street, Nangang, Harbin, Heilongjiang 150000, P.R. China
E-mail: anngan_ag@163.com

Introduction

Osteosarcoma is a malignant tumor originating from mesenchymal tissues (1). It is one of the most common primary tumors, especially in adolescents aged 10 to 20 years (2). Osteosarcoma is highly malignant, with pulmonary metastasis occurring in approximately 85-90% of patients with osteosarcoma (3,4). In recent years, with the in-depth research on the pathogenesis and improvement of osteosarcoma therapies, the 5-year survival rate of localized osteosarcoma has been increased to 60-70% (5), but the 5-year survival rate of metastatic osteosarcoma is only 20-30% (6). In recent years, with the development of tissue engineering, increasing attention has been paid to the development of bone substitutes with custom-made microarchitecture and physicomechanical properties comparable to native bone, such as bioactive three-dimensional (3D) porous polymer or ceramic scaffolds or its conjugated forms, which can mimic the host tissue to facilitate the transferring of nutrients to ensure defective bone restoration (7-9). Moreover, 3D-printed multifunctional polyetheretherketone bone scaffold was widely applied in the multimodal treatment of osteosarcoma and osteomyelitis (10). Clinical results reveal that the efficacy of current chemotherapy drugs in patients with metastatic osteosarcoma is insufficient (11). Thus, the research and development of new therapeutic drugs are deemed significant for the treatment of osteosarcoma at this stage. It has become a top priority to clarify the mechanism of the occurrence and development of osteosarcoma and find effective drug treatments.

Daphne genkwa Sieb. et Zucc. (*Daphne genkwa*), a traditional Chinese herb, was first recorded in Shennong's Classic Materia Medica (12). It is widely grown in China, Japan and other countries (13). *Daphne genkwa* has long been used as an anti-inflammatory, analgesic and sedative drug for edema and asthma (14,15). Hydroxygenkwanin (HGK) is a flavonoid compound extracted from the flower buds of *Daphne genkwa*, which is considered to be one of the active ingredients in *Daphne genkwa* flowers (16). The pharmacological effect of HGK has attracted the attention of researchers and is now widely used in the treatment of various tumors (17,18). Unfortunately, the study of HGK in osteosarcoma has not received much attention.

MicroRNAs (miRNAs or miRs; endogenous non-coding small RNAs) can modify gene expression in eukaryotic cells at post-transcriptional levels (19). Several studies have revealed that ~3% of human genes encode miRNA synthesis, and ~60% of human genes are regulated by miRNAs (20,21). In recent years, the importance of miRNAs in human diseases has been highlighted. miRNAs have therefore become a hotspot in the research of diseases. Similarly, in osteosarcoma, miRNAs also act as regulators and influence the progression of osteosarcoma (22). Among them, upregulation of miR-320a has been revealed to inhibit the proliferation and migration of osteosarcoma (23,24). SRY-box transcription factor 9 (SOX9) is a key transcription factor in chondrocytes (25). Current studies have revealed that SOX9 plays a critical role in the migration and invasion of osteosarcoma cells (26-29). In addition, it is worth noting that from a bioinformatics perspective, miRNA-320a appears to be associated with SOX9. A study on liver cancer from Chou *et al* revealed that HGK could inhibit the metastasis and invasion of hepatocellular carcinoma by promoting the expression of miR-320a (11). Therefore, it was surmised that HGK may regulate the proliferation, invasion and migration of osteosarcoma cells through the miR-320a/SOX9 axis.

In the present study, the effect of HGK on osteosarcoma was detected by treating osteosarcoma cell lines with HGK. The specific molecular mechanism of HGK in the treatment of osteosarcoma was further elucidated by exploring the regulatory effect of HGK on the miR-320a/SOX9 axis. The present study lays a theoretical foundation for the treatment of osteosarcoma by HGK, and also provides a potential targeted drug for the treatment of osteosarcoma.

Materials and methods

Cell culture. Human osteoblasts (hFOB 1.19; cat. no. CRL-11372) and osteosarcoma cells (MG-63; cat. no. CRL-1427; and U2OS; cat. no. HTB-96) were obtained from American Type Culture Collection (ATCC) and cultured in Dulbecco's modified Eagle's medium (DMEM; cat. no. 12491-015) supplemented with 10% fetal bovine serum (FBS; cat. no. 10099-141), 100 U/ml penicillin and 100 μg/ml streptomycin (cat. no. 15070063; all from Gibco; Thermo Fisher Scientific, Inc.) in an incubator at 37˚C with 5% CO_2.

Hydroxygenkwanin (HGK; purity >99%) was purchased from ChemFaces. Various concentrations (0, 10, 20, 40 and 60 μmol/l) of HGK were applied to treat hFOB 1.19 cells to test the safety of the drug. In addition, MG-63 and U2OS cells were also treated with various concentrations of HGK (10, 20, 40 and 60 μmol/l) for 48 h, and assigned as the treatment groups. Moreover, MG-63 and U2OS cells as well as hFOB 1.19 cells received 0 μmol/l HGK and were assigned as the control groups.

3-(4,5-Dimethylthiazol-2-yl)-2,5-diphenyltetrazolium romide (MTT) assay. The cells of each cell line were seeded in a 96-well plate at a density of 1×10^3 cells/well. After the indicated treatments for 48 h, 10 μl MTT solution (cat. no. ST316; Beyotime Institute of Biotechnology) was added to the cells at 37˚C for 4 h. The medium containing MTT was then removed and 200 μl dimethyl sulfoxide (DMSO; cat. no. ST1276; Beyotime Institute of Biotechnology) was added into each well.

Following brief slight shaking, the optical density (OD) value of each well was measured at a wavelength of 490 nm with a microplate reader (Molecular Devices, LLC). Relative cell viability was calculated according to the following formula: Cell relative viability (%)=OD (test)/OD (control) x100%.

Colony formation assay. The cells of MG-63 and U2OS cell lines were seeded in a 6-well plate at a density of 100 cells/well. Next, the cells of each well were treated with various concentrations of HGK (0, 10, 20 and 40 μmol/l), and the medium was changed every 2 days. After 14 days, the cells were fixed with 4% paraformaldehyde (cat. no. P0099; Beyotime Institute of Biotechnology) for 30 min at room temperature. Subsequently, the cells were stained with 0.1% crystal violet (cat. no. C0121; Beyotime Institute of Biotechnology) for 15 min at room temperature. Finally, cell clones were captured with a camera (EOS 3000D; Canon, Inc.) and clones with a cell count >50 were recorded.

Wound healing assay. Treated or untreated MG-63 and U2OS cells were seeded in a 6-well plate at a density of 2×10^5 cells/well. The wound healing assay was carried out when the cell confluence reached 90%. The specific procedure of the assay was as follows: Cells were scratched vertically with a pipette, and then the scratched cells were washed with phosphate-buffered saline (PBS; cat. no. C0221A; Beyotime Institute of Biotechnology). Subsequently, the cells were cultured in a serum-free medium containing HGK (10, 20 and 40 μmol/l). At 0 and 48 h, images of the cells were captured with an inverted microscope at a magnification of x100, and the width of the scratch was measured. The relative migration rate was calculated as follows: Relative migration rate=(0 h scratch width-48 h scratch width)/0 h scratch width x100%.

Transwell assay. The culture plate used in the Transwell assay was an 8-μm pore Transwell plate (product no. 3428, Corning, Inc.). Prior to the initiation of assay, the upper chamber of the Transwell plate was coated with 1:4 diluted BD Matrigel Matrix (cat. no. 356234; BD Biosciences) at 37˚C for 4 h. The treated or untreated MG-63 and U2OS cells (2×10^4) were resuspended in a serum-free medium and then transferred to the upper chamber of the Transwell plate while the corresponding dose of drug (10, 20 or 40 μmol/l HGK) was added. A medium containing 20% FBS was then placed into the lower chamber of the Transwell plate. The Transwell plate was cultured in an incubator for 48 h at 37˚C. After the Transwell upper chamber was removed, the invasive cells were fixed with 4% paraformaldehyde for 15 min at 4˚C and then stained with 0.1% crystal violet staining solution at room temperature for 30 min. Following staining, the invaded cells were counted under an inverted microscope at a magnification of x250 and the relevant results were recorded.

Reverse transcription-quantitative polymerase chain reaction (RT-qPCR). Total RNA from hFOB 1.19, MG-63 and U2OS cells was isolated using TRIzol reagent (cat. no. 15596-018; Invitrogen; Thermo Fisher Scientific, Inc.). The total RNA was subjected to reverse transcription (PrimeScript™ RT reagent kit; cat. no. RR037A; Takara Bio, Inc.) and the product was triply diluted with double distilled

Table I. Specific primer sequences for RT-quantitative polymerase chain reaction.

Gene	Primer sequence	Species
SOX9	Forward: 5'-AGCGAACGCACATCAAGAC-3'	Human
	Reverse: 5'-CTGTAGGCGATCTGTTGGGG-3'	
GAPDH	Forward: 5'-CCACTCCTCCACCTTTGAC-3'	Human
	Reverse: 5'-ACCCTGTTGCTGTAGCCA-3'	
miR-320a	5'-CTCAACTGGTGTCGTGGAGTCG	Human
	GCAATTCAGTTGAGCGGAAGA-3' (RT)	
	Forward: 5'-TCGGCAGGGCCTTCTCTTCCCG-3'	
	Reverse: 5'-CAGTGCAGGGTCCGAGGT-3'	
U6	5'-GTTGGCTCTGGTGCAGGGTCCGAGGTATTCGC	Human
	ACCAGAGCCAACAAAATATGG-3' (RT)	
	Forward: 5'-CTCGCTTCGGCAGCACA-3'	
	Reverse: 5'-AACGCTTCACGAATTTGCGT-3'	

SOX9, SRY-box transcription factor 9; miR-320a, microRNA-320a; RT, reverse transcription.

water. RT-qPCR was then applied to detect the expression levels of SOX9 and miR-320a using the TB Green® Premix Ex Taq™ II kit (cat. no. RR820A) and Mir-X miRNA qRT-PCR TB Green Kit (cat. no. 638314; both from Takara Bio, Inc.), respectively, and an ABI StepOnePlus™ system (Applied Biosystems; Thermo Fisher Scientific, Inc.). The primers used in this experiment were provided by Sangon Biotech Co., Ltd. and are listed in Table I. GAPDH was the internal reference of SOX9 and U6 was the internal reference of miR-320a. The reaction system was as follows: 2 μl cDNA, 10 μl SYBR, 0.8 μl primers and 6.4 μl double distilled water. The thermocycling conditions were as follows: 95˚C for 30 sec, 40 cycles at 95˚C for 3 sec and 60˚C for 30 sec. The RT-qPCR data were analyzed using the $2^{-\Delta\Delta Cq}$ method (30).

Western blot analysis. Total proteins from treated or untreated MG-63 and U2OS cells were extracted with the RIPA reagent (cat. no. P0013B) containing 1% protease inhibitor (P1030; both from Beyotime Institute of Biotechnology). Next, the total protein concentration was determined by a BCA protein kit (cat. no. P0012; Beyotime Institute of Biotechnology). Subsequently, equal amounts of total protein (30 μg of protein per lane) were separated on a 12% gel using SDS-PAGE (cat. no. P0012A; Beyotime Institute of Biotechnology). Following electrophoresis the samples were transferred to a PVDF membrane (ISEQ00010/IPVH00010; Millipore; Merck KGaA). The membrane was sealed with 5% skim milk (cat. no. D8340; Beijing Solarbio Science & Technology Co., Ltd.) and incubated with the primary antibodies at 4˚C overnight, including those against N-cadherin (product no. 14215; 1:1,000) and E-cadherin (product no. 14472; 1:1,000; both from Cell Signaling Technology, Inc.), vimentin (product code ab92547; 1:3,000), SOX9 (product code ab185966; 1:5,000) and GAPDH (product code ab8245; 1:5,000; all from Abcam). The following day, the membrane was incubated with the secondary antibodies: Goat anti-mouse IgG H&L (HRP) (product code ab6789; 1:5,000) and goat anti-rabbit IgG H&L (HRP) (product code ab6721; 1:10,000; both from Abcam) at room temperature for 1 h. The bands were visualized using enhanced chemiluminescence (ECL) solution (cat. no. WBKLS0500; Millipore; Merck KGaA) and BioRad Gel Imager (Bio-Rad Laboratories, Inc.). The intensity of each band was quantified using Image J 1.50i software (National Institutes of Health).

Cell transfection. The cells were seeded in a 6-well plate at a density of 2x10⁵ cells/well. When the cell confluence reached ~80%, the cell transfection was started. MiR-320a mimic (product no. miR10000510-1-5; sense, 5'-AAAAGC UGGGUUGAGAGGGCGA-3' and antisense, 5'-GCCCUC UCAACCCAGCUUUUUU-3'), miR-320a inhibitor (product no. miR20000510-1-5; 5'-UCGCCCUCUCAACCCAGC UUUU-3'), mimic control (product no. miR1N0000001-1-10; sense, 5'-UUCUCCGAACGUGUCACGUTT-3' and antisense, 5'-ACGUGACACGUUCGGAGAATT-3') and inhibitor control (product no. miR2N0000001-1-10; 5'-CAGUACUUU UGUGUAGUACAA-3') were all obtained from Guangzhou RiboBio Co., Ltd. The overexpressed plasmid of SOX9 was constructed via inserting the sequence of SOX9 into the pcDNA 3.1 vector, with the empty vector of pcDNA 3.1 as the negative control (NC). The design and construction of the overexpressed plasmid of SOX9 were completed by Shanghai GenePharma Co., Ltd. The transfection reagent Lipofectamine 2000 (cat. no. 11668-027) used in this experiment was purchased from Invitrogen; Thermo Fisher Scientific, Inc. and cell transfection was performed according to the manufacturer's instructions. Specifically, 10 μl transfection reagent and 4 μg miR-320a mimic, inhibitor, overexpressed plasmid of SOX9 or their control were diluted with 250 μl Opti-MEM (cat. no. 31985-070; Gibco; Thermo Fisher Scientific, Inc.), respectively. After standing for 5 min, the mixtures were remixed. After standing again for 20 min, the corresponding cells were added for transfection for 48 h at 37˚C. At 48 h post-transfection, RT-qPCR was used to measure the transfection efficiency.

Bioinformatic analyses and dual luciferase reporter assay. The targeted binding sites of miR-320a and SOX9 were predicted by starBase v2.0 (https://starbase.sysu.edu.cn/starbase2/index.php). The 3'-untranslated region (UTR) sequence of SOX9 gene was obtained from NCBI (https://www.ncbi.nlm.nih.gov/). The SOX9 wild-type sequence (5'-gagaagcauuugguaAGCUUUa-3') and the mutant sequence (the mutant site was the miR-320a-binding region) (5'-gagaagcauuugguaUACACUa-3') were then constructed into the pmirGLO plasmid (cat. no. E1330; Promega Corporation), named SOX9-WT and SOX9-MUT. Afterwards, the SOX9-WT or SOX9-MUT plasmid and miR-320a mimic or mimic control were co-transfected into MG63 and U2OS cells. Subsequently, cells were transfected using Lipofectamine 2000 (cat. no. 11668-027; Invitrogen; Thermo Fisher Scientific, Inc.) according to the method described above. After 24 h, the fluorescence intensity of cells in each group was detected by Dual Luciferase Reporter gene detection system (cat. no. E1910; Promega Corporation). Renilla luciferase activity was used to normalize Firefly luciferase activity.

Xenograft assays. A total of 10 male, 6-week-old BALB/c nude mice (Weitong Lihua Laboratory Animal Technology Co., Ltd.) were used to study the antitumor activity of HGK against osteosarcoma. The BALB/c nude mice were kept at 24-26°C and in 40-70% humidity, with a 12-h light/dark cycle and free access to food and water. BALB/c nude mice were divided into control and HGK groups (n=5, each group), and the animals were inoculated subcutaneously in the right flank with MG-63 cells ($3x10^6$) in 100 μl. Drug treatment was started on day 10, where the nude mice in the HGK group were intraperitoneally injected with 100 μl HGK (1.0 mg/kg body weight) every two days, and the control group was treated with an equal volume of PBS. The tumor volume was measured according to the following formula: Tumor volume=length x width^2/2. After 4 weeks, these nude mice were sacrificed by cervical dislocation following anesthesia with an intraperitoneal injection of sodium pentobarbital (60 mg/kg), and then the tumors were photographed, and the weight was measured. The maximum allowed tumor size did not exceed 1,000 mm^3. The study was approved by the Animal Ethics Committee of Nanfang Hospital (Guangzhou, China; approval no. NFYY-2021-121).

Statistical analysis. GraphPad Prism 8.0 (GraphPad Software, Inc.) was employed for statistical analysis. Each experiment was repeated three times. Data are presented as the mean ± standard deviation. Unpaired t-test was utilized for comparison between two groups, while one-way analysis of variance (ANOVA) and Tukey's post hoc test were used for comparison among multiple groups. P<0.05 was considered to indicate a statistically significant difference.

Results

HGK suppresses the proliferation, migration and invasion of osteosarcoma cells. The chemical structure formula of HGK is presented in Fig. 1A. In order to test the safety of HGK, hFOB1.19 (an immortalized human fetal osteoblastic cell line) was first treated with various concentrations of HGK (0, 10, 20, 40 and 60 μmol/l), and the results revealed that HGK had no significant effect on hFOB1.19 cells (P>0.05; Fig. 1B). This suggested that HGK within a concentration of 60 μmol/l exerted no toxic effect on normal osteoblasts. Similarly, osteosarcoma cells MG-63 and U2OS were treated with various concentrations of HGK as well. As demonstrated in Fig. 1C and D, HGK decreased the viability of MG-63 and U2OS cells in a concentration-dependent manner as compared with the control group (P<0.05 and P<0.001). From the results, it was determined that the half-maximal lethal concentration of HGK was ≤40 μmol/l, thus, the concentrations of 10, 20 and 40 μmol/l were selected for the subsequent experiments. The effects of HGK on the proliferation, migration and invasion of MG-63 and U2OS cells were then also evaluated. Colony formation assay revealed that the cell proliferation in the HGK groups was reduced compared with the control group (Fig. 1E-H; P<0.05, P<0.01 and P<0.001). In addition, the wound healing assay demonstrated that the migration of cells in the HGK groups was diminished compared with the control group (Fig. 2A-D; P<0.01 and P<0.001). Moreover, Transwell assays revealed that the invasion of cells in the HGK groups was decreased compared with the control group (Fig. 2E-H; P<0.01 and P<0.001). All these results indicated that HGK inhibited cell proliferation, migration and invasion in a concentration-dependent manner.

HGK inhibits the proliferation, migration and invasion of osteosarcoma cells by promoting the expression of miR-320a. The expression of miR-320a in osteosarcoma cells was lower than that in osteoblasts (Fig. 3A; P<0.001). Further detection revealed that HGK could promote the expression of miR-320a in MG-63 and U2OS cells in a concentration-dependent manner (Fig. 3B and C; P<0.001). To verify the effects of HGK and miR-320a on osteosarcoma cells, a miR-320a inhibitor was used to decrease the expression of miR-320a. The transfection efficiency of miR-320a inhibitor is presented in Fig. 3D and E (P<0.001). Moreover, it was also determined that miR-320a inhibitor could reverse the promotive effect of HGK on miR-320a expression (Fig. 3F and G; P<0.01 and P<0.001). Next, the effects of HGK and miR-320a inhibitor on proliferation, migration and invasion of MG-63 and U2OS cells were assessed. The results of the colony formation assays suggested that the proliferation of cells in the miR-320a inhibitor group was increased compared with the control group (Fig. 3H-J; P<0.001). Moreover, miR-320a inhibitor could reverse the inhibitory effect of HGK on cell proliferation (Fig. 3H-J; P<0.001). Wound healing assay revealed that cell migration in the miR-320a inhibitor group was increased compared with the control group (Fig. 4A-D; P<0.001). Similarly, miR-320a inhibitor could reverse the inhibitory effect of HGK on the cell migration (Fig. 4A-D; P<0.001). The Transwell assay demonstrated that cell invasion in the miR-320a inhibitor group was promoted compared with the control group (Fig. 4E-H; P<0.001). In addition, miR-320a inhibitor could also reverse the effect of HGK on cell invasion (Fig. 4E-H; P<0.001).

HGK inhibits the expression of SOX9 by promoting miR-320a expression. The targeted binding sites of miR-320a and SOX9 were first predicted by starBase v2.0 (Fig. 5A). Subsequently,
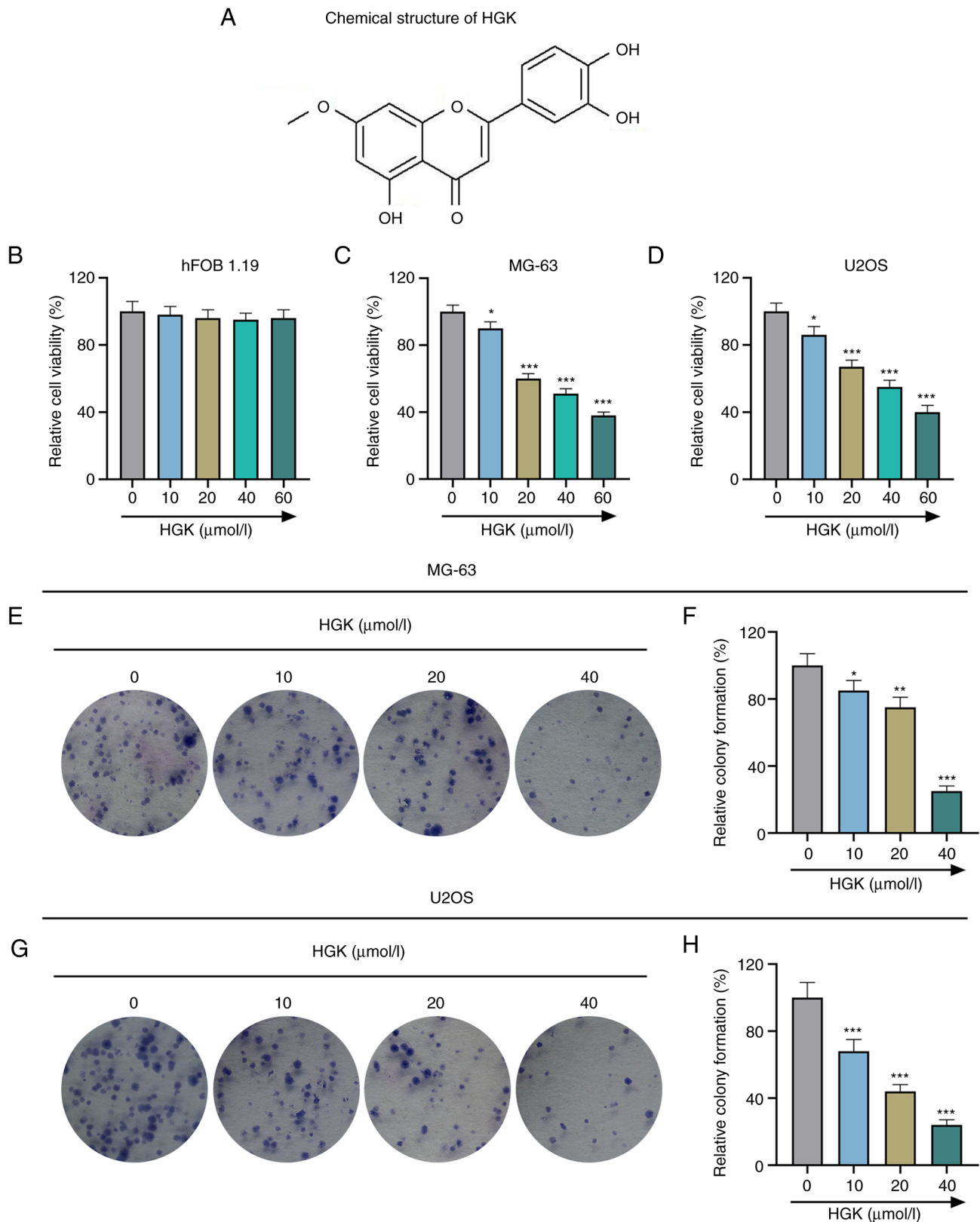
Figure 1. HGK decreases the viability and proliferation of MG-63 and U2OS cells. (A) The chemical structure of HGK. (B) The cell viability of hFOB 1.19 cells treated or untreated with HGK was detected by MTT assay. (C and D) The cell viability of MG-63 and U2OS cells treated or untreated with HGK was determined by MTT assay. (E-H) The cell proliferation of MG-63 and U2OS cells treated or untreated with HGK was assessed using colony formation assay. *P<0.05, **P<0.01 and ***P<0.001 vs. 0 µmol/l. HGK, hydroxygenkwanin; MTT, 3-(4,5-dimethylthiazol-2-yl)-2,5-diphenyltetrazolium bromide.

a dual-luciferase reporter assay revealed that the fluorescence intensity of cells in the SOX9-WT + miR-320a mimic group was significantly lower than that in the mimic control group (Fig. 5B; P<0.01), while the fluorescence intensity in the SOX9-MUT + miR-320a mimic group displayed no significant change compared to that in the mimic control group
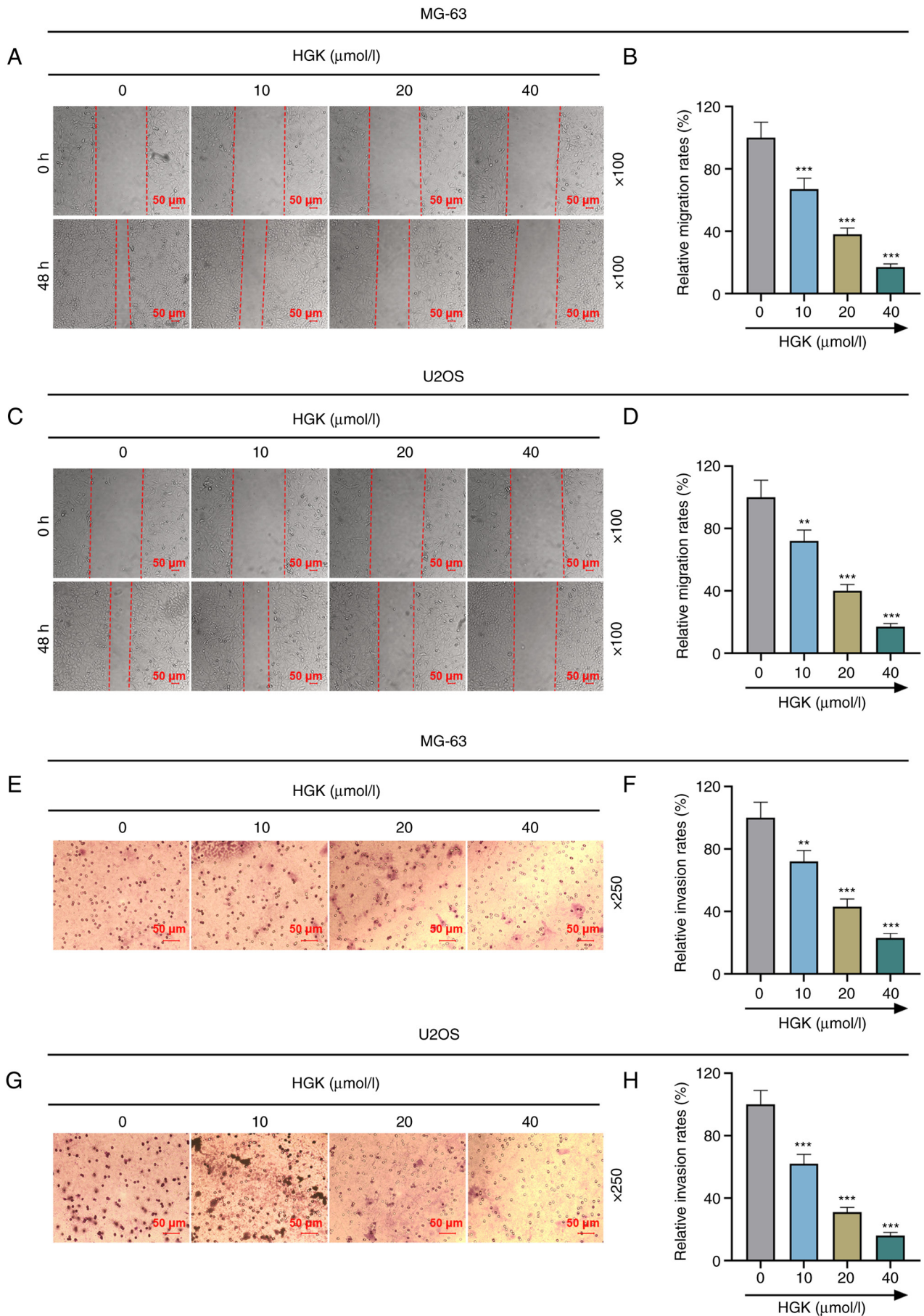
Figure 2. HGK decreases the migration and invasion of MG-63 and U2OS cells. (A-D) The cell migration of MG-63 and U2OS cells treated or untreated with HGK was assessed by wound healing assay. Magnification, x100. (E-H) The cell invasion of MG-63 and U2OS cells treated or untreated with HGK was assessed by Transwell assay. Magnification, x250. **P<0.01 and ***P<0.001 vs. 0 μmol/l. HGK, hydroxygenkwanin.
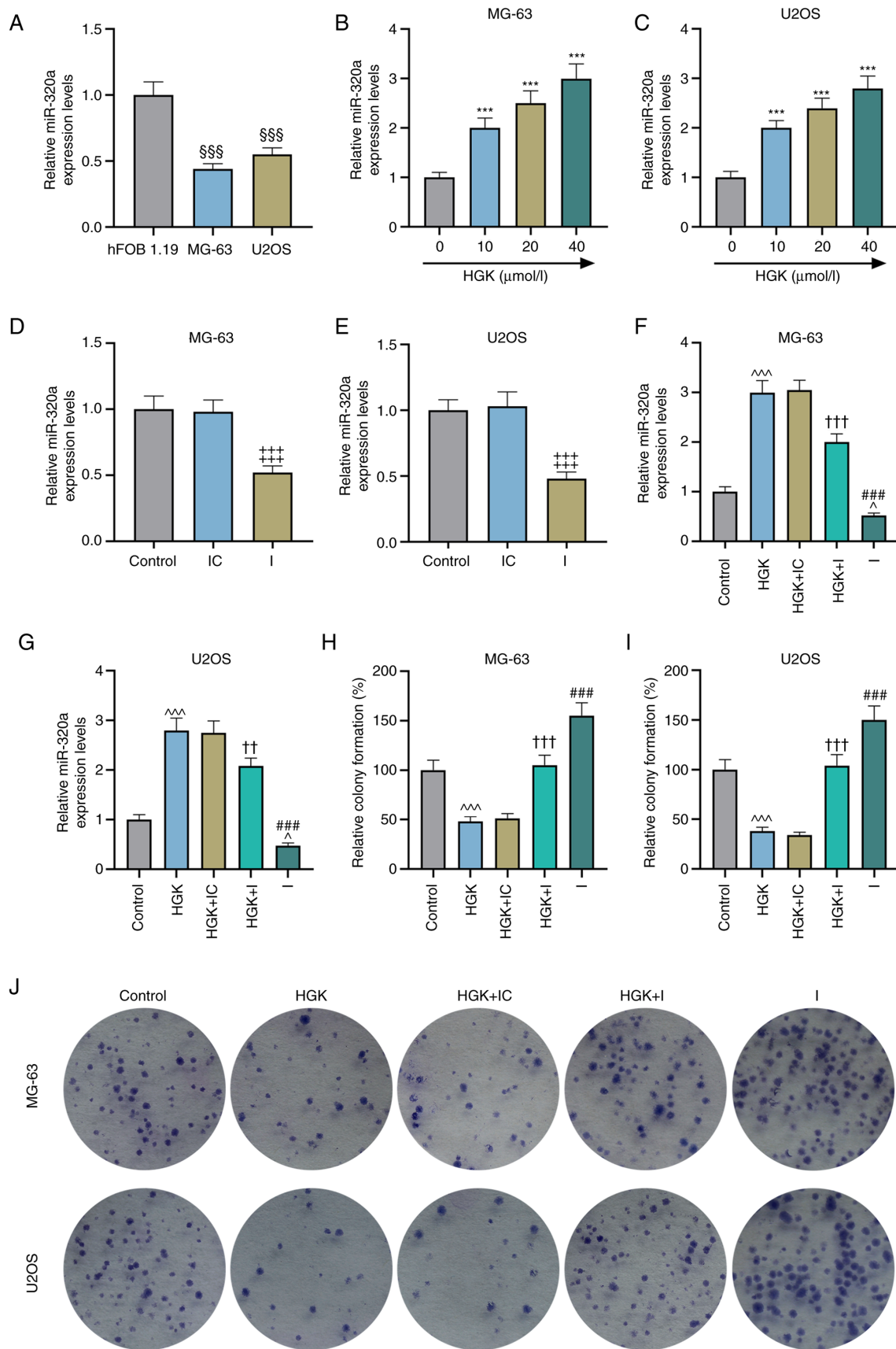
Figure 3. HGK decreases the proliferation of MG-63 and U2OS cells by promoting miR-320a expression. (A) The expression of miR-320a in hFOB 1.19, MG-63 and U2OS cells was quantified by RT-qPCR. (B and C) The expression of miR-320a in MG-63 and U2OS cells treated or untreated with HGK was detected by RT-qPCR. (D and E) Transfection efficiency of miR-320a inhibitor in MG-63 and U2OS cells was evaluated by RT-qPCR. (F and G) The expression of miR-320a in MG-63 and U2OS cells treated or untreated with HGK and/or miR-320a inhibitor was determined by RT-qPCR. (H-J) The cell proliferation of MG-63 and U2OS cells treated or untreated with HGK and/or miR-320a inhibitor was examined by colony formation assay. $^{§§§}P<0.001$ vs. hFOB 1.19; $^{***}P<0.001$ vs. 0 μmol/l; $^{‡‡‡}P<0.001$ vs. IC; $^{^}P<0.05$ and $^{^^^}P<0.001$ vs. Control; $^{††}P<0.01$ and $^{†††}P<0.001$ vs. HGK + IC; $^{###}P<0.001$ vs. HGK + I. HGK, hydroxygenkwanin; miR-320a, microRNA-320a; RT-qPCR, reverse transcription-quantitative polymerase chain reaction; I, miR-320a inhibitor; IC, miR-320a inhibitor control.
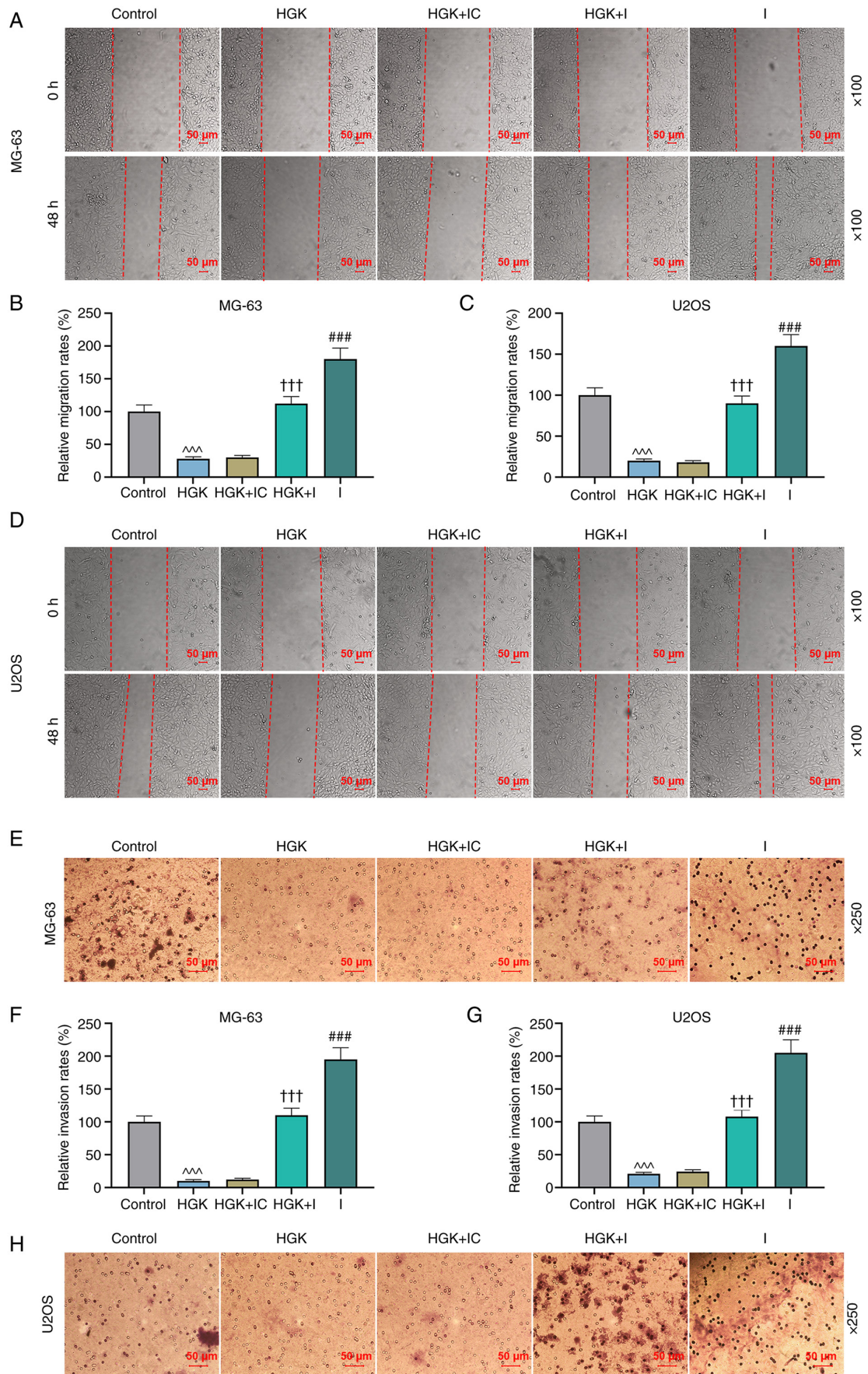
Figure 4. HGK decreases the migration and invasion of MG-63 and U2OS cells by promoting miR-320a expression. (A-D) The cell migration of MG-63 and U2OS cells treated or untreated with HGK and/or miR-320a inhibitor was detected by wound healing assay. Magnification, x100. (E-H) The cell invasion of MG-63 and U2OS cells treated or untreated with HGK and/or miR-320a inhibitor was assessed by Transwell assay. Magnification, x250. ^^^P<0.001 vs. Control; †††P<0.001 vs. HGK + IC; ###P<0.001 vs. HGK + I. HGK, hydroxygenkwanin; miR-320a, microRNA-320a; I, miR-320a inhibitor; IC, miR-320a inhibitor control.
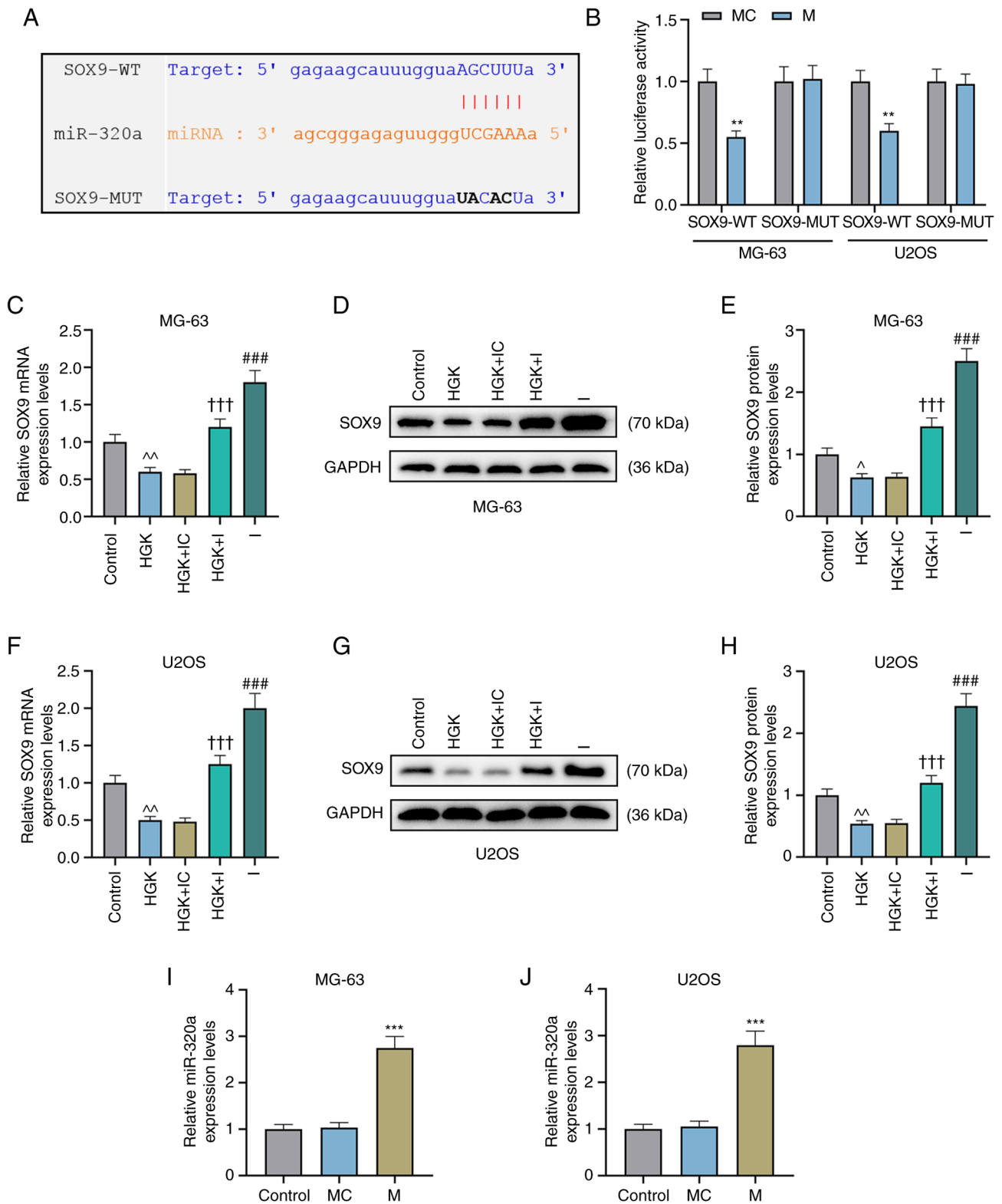
Figure 5. HGK decreases SOX9 expression by promoting miR-320a expression in MG-63 and U2OS cells. (A) starBase predicted the binding site of miR-320a and SOX9. (B) Dual luciferase reporter assay was employed to verify the targeted bindings of miR-320a and SOX9. (C-H) The expression of SOX9 in MG-63 and U2OS cells treated or untreated with HGK and/or miR-320a inhibitor was quantified by RT-qPCR and western blotting. (I and J) Transfection efficiency of miR-320a mimic in MG-63 and U2OS cells was evaluated by RT-qPCR. **P<0.01 and ***P<0.001 vs. MC; ^P<0.05 and ^^P<0.01 vs. Control; †††P<0.001 vs. HGK + IC; ###P<0.001 vs. HGK + I. HGK, hydroxygenkwanin; SOX9, SRY-box transcription factor 9; miR-320a, microRNA-320a; RT-qPCR, quantitative reverse transcription polymerase chain reaction; M, miR-320a mimic; MC, miR-320a mimic control; IC, miR-320a inhibitor control; I, miR-320a inhibitor.

(Fig. 5B). This indicated that miR-320a indeed targeted SOX9. Further study demonstrated that the expression of SOX9 was depleted in the HGK group compared with the control group (Fig. 5C-H; P<0.05 and P<0.01). However, miR-320a inhibitor could abolish the inhibitory effect of HGK on SOX9 expression (Fig. 5C-H; P<0.001).
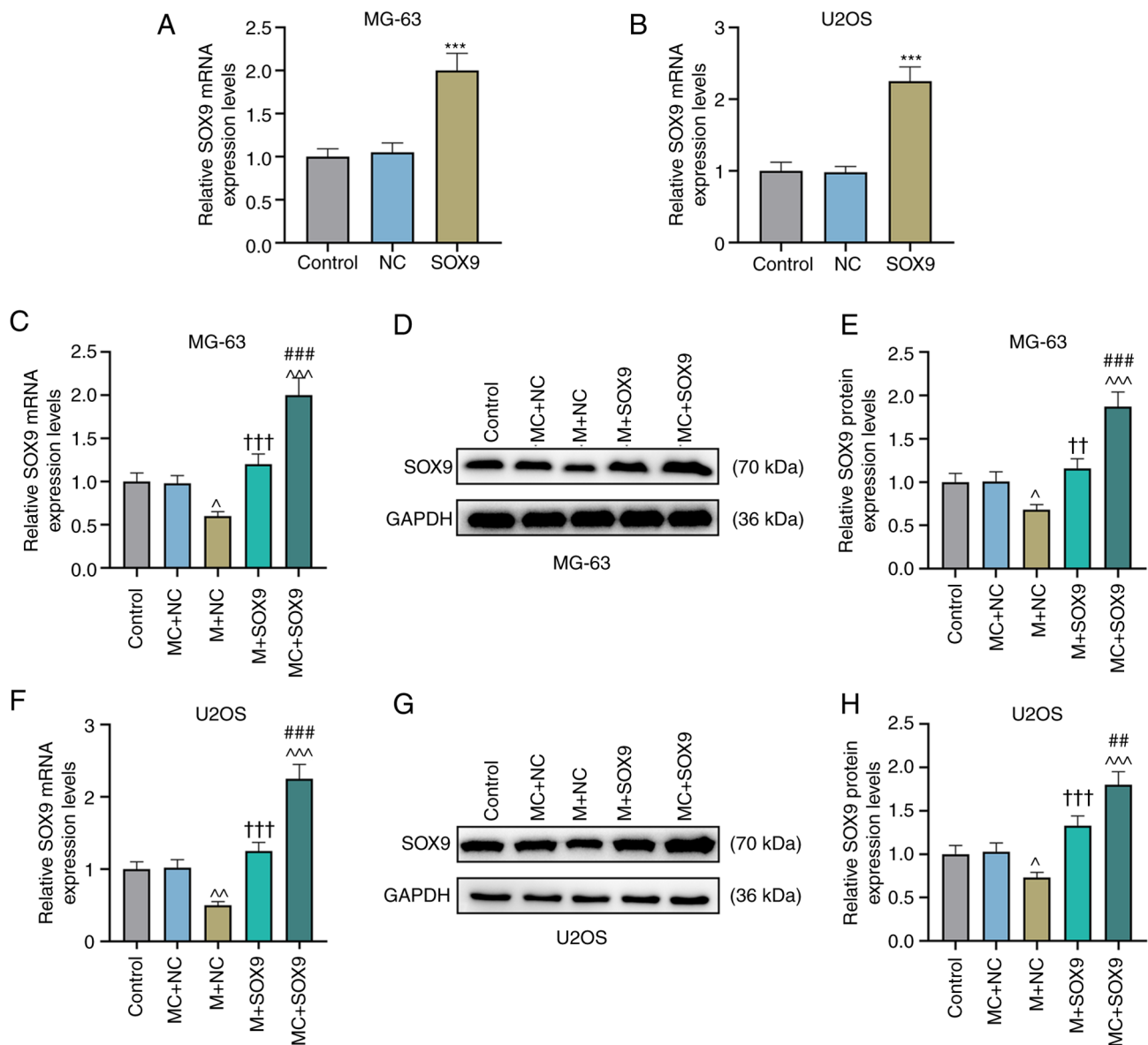
Figure 6. MiR-320a decreases the expression of SOX9 in MG-63 and U2OS cells. (A and B) Transfection efficiency of SOX9 overexpression plasmid in MG-63 and U2OS cells was assessed by RT-qPCR. (C-H) The expression of SOX9 in MG-63 and U2OS cells transfected or untransfected with miR-320a mimic and/or SOX9 overexpression plasmid was quantified by RT-qPCR and western blotting. ***$P<0.001$ vs. NC; ^$P<0.05$, ^^$P<0.01$ and ^^^$P<0.001$ vs. MC + NC; ††$P<0.01$ and †††$P<0.001$ vs. M + NC; ##$P<0.01$ and ###$P<0.001$ vs. M + SOX9. MiR-320a, microRNA-320a; SOX9, SRY-box transcription factor 9; RT-qPCR, reverse transcription-quantitative polymerase chain reaction; NC, negative control; MC, miR-320a mimic control; M, miR-320a mimic.

MiR-320a inhibits the migration, invasion and epithelial-mesenchymal transition (EMT)-related protein expression levels of osteosarcoma cells by inhibiting the expression of SOX9. In order to further assess the effect of the miR-320a/SOX9 axis on osteosarcoma, miR-320a mimic was used to promote the expression of miR-320a (Fig. 5I and J; $P<0.001$). Concurrently, SOX9 overexpressed plasmid was also employed to upregulate the expression of SOX9 (Fig. 6A and B; $P<0.001$). It was then determined that the expression of SOX9 was inhibited in the miR-320a mimic + NC group as compared with the MC + NC group (Fig. 6C-H; $P<0.05$ and $P<0.01$). Subsequently, the effect of miR-320a/SOX9 on the migration and invasion of osteosarcoma cells was examined. As demonstrated in Fig. 7A-D, the migration of MG-63 and U2OS cells was enhanced in the MC + SOX9 group compared with the MC + NC group ($P<0.05$, $P<0.01$ and $P<0.001$). In

addition, SOX9 could reverse the effect of miR-320a mimic on the migration of MG-63 and U2OS cells (Fig. 7A-D; $P<0.05$ and $P<0.01$). According to Fig. 7E-H, the invasion of MG-63 and U2OS cells was promoted in MC + SOX9 group, compared with the MC + NC group ($P<0.001$). In addition, SOX9 could reverse the effect of miR-320a mimic on the invasion of MG-63 and U2OS cells (Fig. 7E-H; $P<0.001$). In order to further confirm the effects of the miR-320a/SOX9 axis on the migration and invasion of cells, EMT-related proteins were also detected. The results revealed that miR-320a mimic could increase the expression of E-cadherin while diminishing the expression levels of N-cadherin and vimentin, compared with those in the MC + NC group (Fig. 8A-D; $P<0.001$). The effects of SOX9 were the opposite of those obtained with the miR-320a mimic (Fig. 8A-D; $P<0.001$). Similarly, upregulation of SOX9 could also reverse the effects of miR-320a mimic on
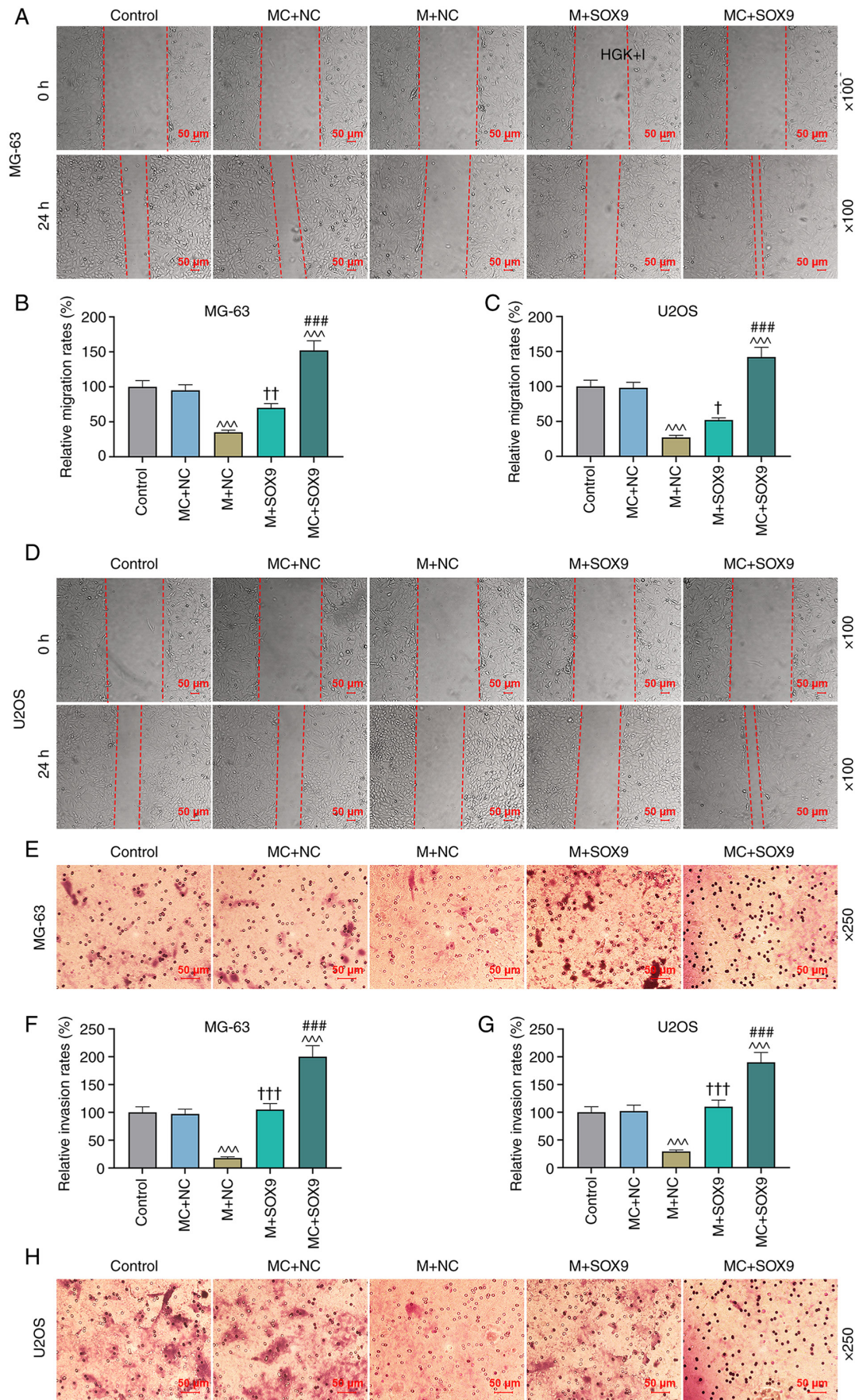
Figure 7. MiR-320a decreases the cell migration and invasion abilities of MG-63 and U2OS cells by inhibiting the expression of SOX9. (A-D) The migration of MG-63 and U2OS cells transfected or untransfected with miR-320a mimic and/or SOX9 overexpression plasmid was detected by wound healing assay. Magnification, x100. (E-H) The cell invasion of MG-63 and U2OS cells transfected or untransfected with miR-320a mimic and/or SOX9 overexpression plasmid was determined by Transwell assay. Magnification, x250. ^^^P<0.001 vs. MC + NC; †P<0.05, ††P<0.01 and †††P<0.001 vs. M + NC; ###P<0.001 vs. M + SOX9. MiR-320a, microRNA-320a; SOX9, SRY-box transcription factor 9; MC, miR-320a mimic control; NC, negative control; M, miR-320a mimic.
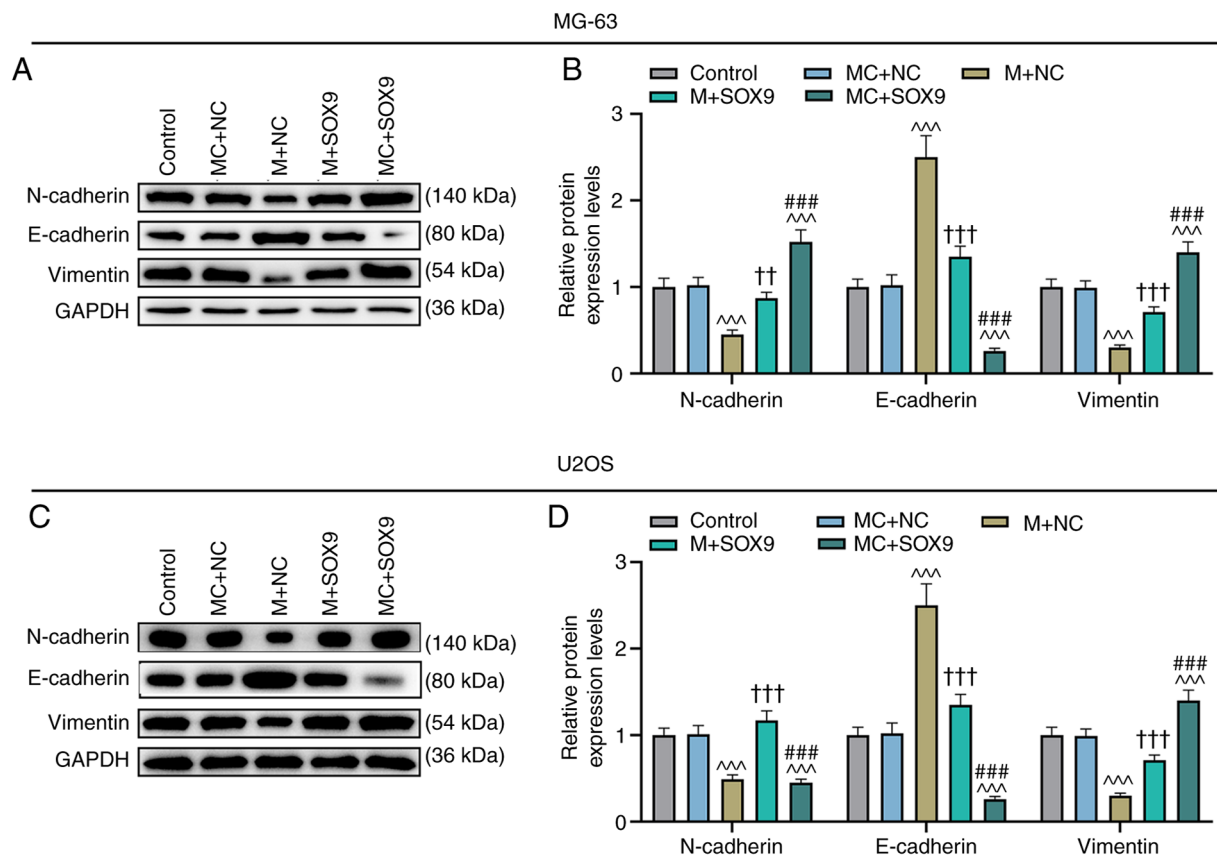
Figure 8. MiR-320a increases E-cadherin expression while decreasing N-cadherin, and vimentin expression levels by inhibiting the expression of SOX9. (A-D) The expression levels of E-cadherin, N-cadherin and vimentin in MG-63 and U2OS cells transfected or untransfected with miR-320a mimic and/or SOX9 overexpression plasmid were detected by western blotting. ^^^$P<0.001$ vs. MC + NC; ††$P<0.01$ and †††$P<0.001$ vs. M + NC; ###$P<0.001$ vs. M + SOX9. MiR-320a, microRNA-320a; SOX9, SRY-box transcription factor 9; MC, miR-320a mimic control; NC, negative control; M, miR-320a mimic.

the expression levels of E-cadherin, N-cadherin and vimentin (Fig. 8A-D; $P<0.01$ and $P<0.001$).

HGK inhibits the osteosarcoma tumor growth of nude mice in vivo. A xenograft mouse model was constructed in the present study to evaluate the antitumor activity of HGK *in vivo.* As revealed in Fig. 9A-C, HGK inhibited the tumor volume and weight in the HGK group compared with the control group.

Discussion

The medicinal value of *Daphne genkwa* dated back to ancient times (31). *Daphne genkwa* is often used to treat edema and make expectoration easy (32). As one of the active ingredients of *Daphne genkwa*, HGK has also been identified to possess powerful biological functions in the treatment of assorted diseases, especially its antitumor effect. For example, Huang *et al* indicated that HGK inhibits the invasion and migration of oral squamous cell cancer cells by downregulating the expression level of vimentin (33). Chen *et al* (17) reported that HGK can inhibit the expression of HDAC to induce the expression of tumor suppressor p21, and promote the acetylation and activation of p53 and p65, thus inhibiting the growth, migration and invasion of liver cancer cells and increasing the cell apoptosis. Notably, this aforementioned study, revealed that the antitumor effect of HGK was mainly demonstrated through the inhibition

of the migration and invasion of tumor cells. It is important to note that the primary cause of mortality for osteosarcoma is pulmonary metastasis, and current chemotherapy regimens appear to be ineffective against metastasis of osteosarcoma (34). The outstanding ability of HGK to suppress migration and invasion makes it a noteworthy potential drug for our research, and indicates that it may be a potential drug for the treatment of osteosarcoma. In the present study, it was revealed that HGK did not affect the viability of normal human osteoblasts, indicating that the safety of HGK was reliable. In addition, further study revealed that HGK could reduce the proliferation, migration and invasion of osteosarcoma cells.

In our subsequent study, it was determined that HGK could promote the expression of miR-320a in osteosarcoma cells. In fact, the role of miR-320a in osteosarcoma has been extensively studied, involving doxorubicin resistance, and its effect on proliferation, migration, and invasion of osteosarcoma cells (23,24,35). In addition, it has been reported that overexpression of miR-320a promotes stress oxidation levels, while reducing the viability, proliferation and mineralization capacities of osteosarcoma cells (36). A previous study even proposed miR-320a as a possible biomarker for osteosarcoma (37). Therefore, it can be theorized that the role of HGK in osteosarcoma may be realized by regulating miR-320a. Notably, a recent study by Chou *et al* revealed that HGK can inhibit tumor progression by promoting the expression of miR-320a in lung cancer (11). Their research adds to the credibility of our theory. In
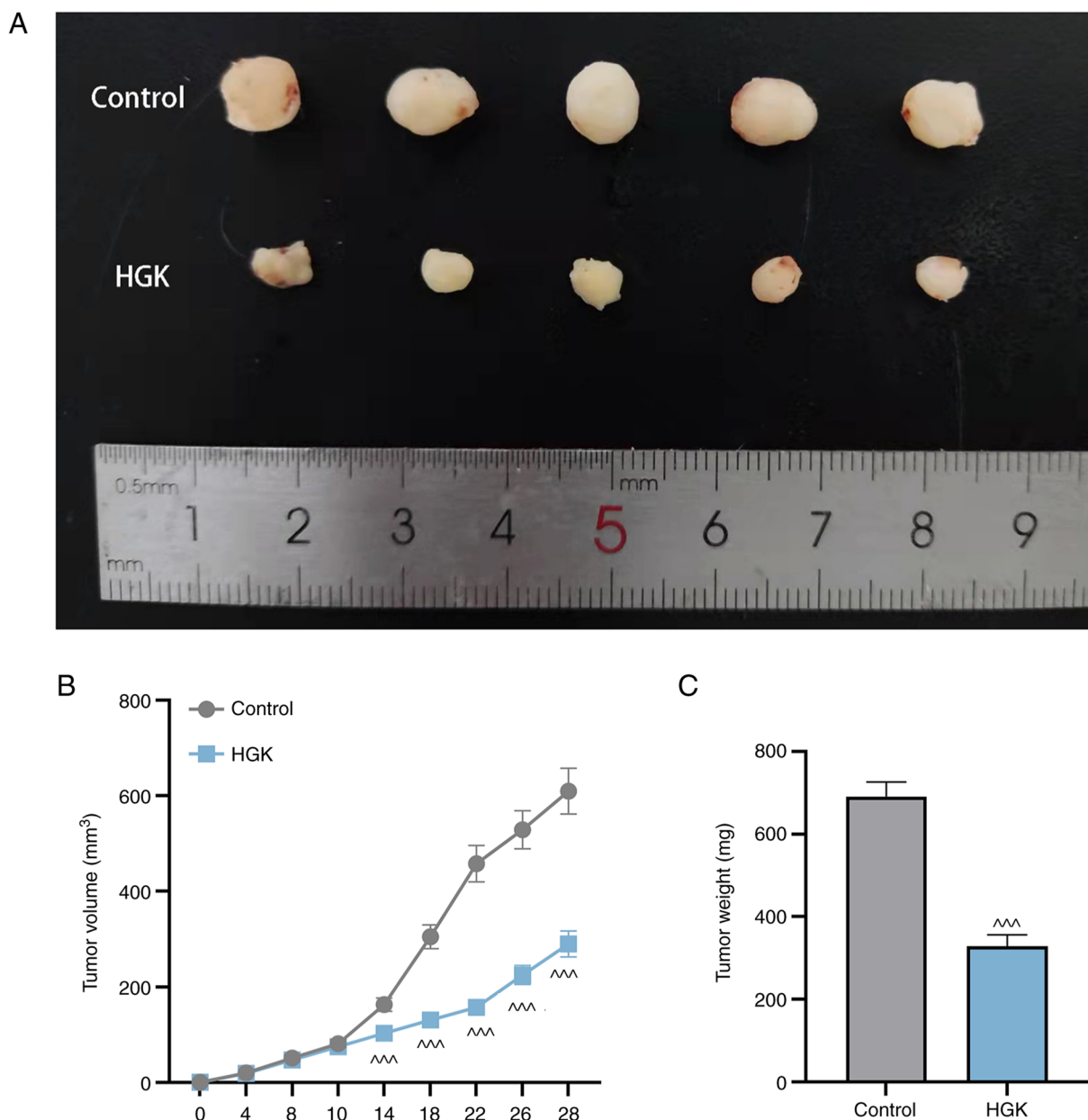
Figure 9. HGK suppresses tumor growth in mice. (A) Tumor images of control and HGK groups (n=5). (B) The effects of HGK treatment on the tumor volume of mice. (C) The effects of HGK treatment on the tumor weight of mice. ^^^$P<0.001$ vs. Control. HGK, hydroxygenkwanin.

order to determine the association between miR-320a and HGK, osteosarcoma cells were treated with HGK and an increased expression of miR-320a was detected. This suggested that HGK had a regulatory effect on miR-320a, but whether it further affected the migration and invasion of osteosarcoma needed to be further explored. MiR-320a inhibitor was used to decrease miR-320a expression, and the aforementioned conjecture was verified by miR-320a inhibitor. The results clearly revealed that HGK-inhibited migration and invasion of osteosarcoma cells were partially counteracted by miR-320a inhibitor.

The starBase database is commonly used to predict the downstream target molecules and targeted binding sites of miRNAs (38). In the present study, the targeted bindings of miR-320a and SOX9 were predicted through starBase database. This result was also confirmed by dual luciferase reporter assay. Notably, SOX9 has been reported to be an essential transcription factor for normal differentiation of osteoblasts and also plays an important role in the progression of osteosarcoma (27,29). In fact, the results of the present study demonstrated that HGK could decrease the expression of SOX9. In addition, miR-320a inhibitor could partially offset the effects of HGK on SOX9 expression. This indicated that HGK can inhibit the expression of SOX9 by promoting miR-320a expression. Further exploration revealed that miR-320a alleviated the migration and invasion abilities of osteosarcoma cells by inhibiting SOX9 expression. These results were further confirmed using western blot analysis. Additionally, EMT has been demonstrated to be an important process of migration and invasion, during which the connexins (such as E-cadherin) are gradually decreased and the expression levels of mesenchymal marker proteins (N-cadherin and vimentin) are promoted in cells (39). The results of the present

study indicated that upregulation of miR-320a could promote the expression of E-cadherin while inhibiting the expression levels of N-cadherin and vimentin. However, overexpression of SOX9 could reverse the regulatory effects of miR-320a on the expression of E-cadherin, N-cadherin and vimentin. Moreover, our results also confirmed that miR-320a decreased the cell migration and invasion of osteosarcoma cells by inhibiting the expression of SOX9. In addition, similar to a previous study (11), the present study revealed that HGK had no significant effect on hFOB1.19 cells, while inhibiting the viability of osteosarcoma cells. This suggested that HGK selectively killed tumor cells without significant toxicity to normal cells. The mechanism revealing how HGK could selectively kill tumor cells remains unclear and needs to be further explored.

Collectively, the present experiments demonstrated that HGK could attenuate the proliferation, migration and invasion of osteosarcoma cells by regulating the miR-320a/SOX9 axis. Unfortunately, our study was only conducted *in vitro*, and further investigation *in vivo* and clinical trials are required. HGK is a potential drug for the treatment of osteosarcoma and is expected to provide a new direction for the clinical research on osteosarcoma.

Availability of data and materials

The analyzed datasets generated during the study are available from the corresponding author on reasonable request.

Authors' contributions

XD made substantial contributions to conception and design of the study. YW, HZ and GA acquired, analyzed and interpreted the data. XD drafted the manuscript and critically revised it for important intellectual content. XD and GA confirm the authenticity of all the raw data. All authors read and approved the final version for the manuscript to be published and agree to be accountable for all aspects of the work in ensuring that questions related to the accuracy or integrity of the work are appropriately investigated and resolved.

Ethics approval and consent to participate

The study was approved by the Animal Ethics Committee of Nanfang Hospital (Guangzhou, China; approval no. NFYY-2021-121). Animal experiments were performed in Nanfang Hospital, which has project co-operation and is linked with the Traditional Chinese Medicine Hospital of Binzhou (Binzhou, China).

Patient consent for publication

Not applicable.

Competing interests

The authors declare that they have no competing interests.

References

1. Mannerström B, Kornilov R, Abu-Shahba AG, Chowdhury IM, Sinha S, Seppänen-Kaijansinkko R and Kaur S: Epigenetic alterations in mesenchymal stem cells by osteosarcoma-derived extracellular vesicles. Epigenetics 14: 352-364, 2019.
2. Brown HK, Tellez-Gabriel M and Heymann D: Cancer stem cells in osteosarcoma. Cancer Lett 386: 189-195, 2017.
3. Gross AC, Cam H, Phelps DA, Saraf AJ, Bid HK, Cam M, London CA, Winget SA, Arnold MA, Brandolini L, *et al*: IL-6 and CXCL8 mediate osteosarcoma-lung interactions critical to metastasis. JCI Insight 3: e99791, 2018.
4. Meazza C and Scanagatta P: Metastatic osteosarcoma: A challenging multidisciplinary treatment. Expert Rev Anticancer Ther 16: 543-556, 2016.
5. Luetke A, Meyers PA, Lewis I and Juergens H: Osteosarcoma treatment-where do we stand? A state of the art review. Cancer Treat Rev 40: 523-532, 2014.
6. Haghiralsadat F, Amoabediny G, Naderinezhad S, Zandieh-Doulabi B, Forouzanfar T and Helder MN: Codelivery of doxorubicin and JIP1 siRNA with novel EphA2-targeted PEGylated cationic nanoliposomes to overcome osteosarcoma multidrug resistance. Int J Nanomedicine 13: 3853-3866, 2018.
7. Sreeja S, Parameshwar R, Varma PRH and Sailaja GS: Hierarchically porous osteoinductive Poly(hydroxyethyl methacrylate-co-methyl methacrylate) scaffold with sustained doxorubicin delivery for consolidated osteosarcoma treatment and bone defect repair. ACS Biomater Sci Eng 7: 701-717, 2021.
8. Xu M, Li H, Zhai D, Chang J, Chen S and Wu C: Hierarchically porous nagelschmidtite bioceramic-silk scaffolds for bone tissue engineering. J Mater Chem B 3: 3799-3809, 2015.
9. Torres AL, Gaspar VM, Serra IR, Diogo GS, Fradique R, Silva AP and Correia IJ: Bioactive polymeric-ceramic hybrid 3D scaffold for application in bone tissue regeneration. Mater Sci Eng C Mater Biol Appl 33: 4460-4469, 2013.
10. Zhu C, He M, Sun D, Huang Y, Huang L, Du M, Wang J, Wang J, Li Z, Hu B, *et al*: 3D-Printed multifunctional polyetheretherketone bone scaffold for multimodal treatment of osteosarcoma and osteomyelitis. ACS Appl Mater Interfaces 13: 47327-47340, 2021.
11. Chou LF, Chen CY, Yang WH, Chen CC, Chang JL, Leu YL, Liou MJ and Wang TH: Suppression of hepatocellular carcinoma progression through FOXM1 and EMT inhibition via hydroxygenkwanin-induced miR-320a expression. Biomolecules 10: 20, 2019.
12. Chen YY, Tang YP, Shang EX, Zhu ZH, Tao WW, Yu JG, Feng LM, Yang J, Wang J, Su SL, *et al*: Incompatibility assessment of genkwa flos and glycyrrhizae radix et Rhizoma with biochemical, histopathological and metabonomic approach. J Ethnopharmacol 229: 222-232, 2019.
13. Li Y, Geng L, Liu Y, Chen M, Mu Q, Zhang X, Zhang Z, Ren G and Liu C: Identification of three Daphne species by DNA barcoding and HPLC fingerprint analysis. PLoS One 13: e0201711, 2018.
14. Wang L, Lan XY, Ji J, Zhang CF, Li F, Wang CZ and Yuan CS: Anti-inflammatory and anti-angiogenic activities in vitro of eight diterpenes from Daphne genkwa based on hierarchical cluster and principal component analysis. J Nat Med 72: 675-685, 2018.
15. Li S, Chou G, Hseu Y, Yang H, Kwan H and Yu Z: Isolation of anticancer constituents from flos genkwa (Daphne genkwa Sieb. et Zucc.) through bioassay-guided procedures. Chem Cent J 7: 159, 2013.
16. Li YN, Yin LH, Xu LN and Peng JY: A simple and efficient protocol for large-scale preparation of three flavonoids from the flower of Daphne genkwa by combination of macroporous resin and counter-current chromatography. J Sep Sci 33: 2168-2175, 2010.
17. Chen CY, Chen CC, Chuang WY, Leu YL, Ueng SH, Hsueh C, Yeh CT and Wang TH: Hydroxygenkwanin inhibits class I HDAC expression and synergistically enhances the antitumor activity of sorafenib in liver cancer cells. Front Oncol 10: 216, 2020.
18. Wang Y, Xu YS, Yin LH, Xu LN, Peng JY, Zhou H and Kang W: Synergistic anti-glioma effect of hydroxygenkwanin and apigenin in vitro. Chem Biol Interact 206: 346-355, 2013.

19. Correia de Sousa M, Gjorgjieva M, Dolicka D, Sobolewski C and Foti M: Deciphering miRNAs' action through miRNA editing. Int J Mol Sci 20: 6249, 2019.
20. Di Leva G, Garofalo M and Croce CM: MicroRNAs in cancer. Annu Rev Pathol 9: 287-314, 2014.
21. Wang S, Lv S, Guan Y, Gao G, Li J, Hei F and Long C: Cardiopulmonary bypass techniques and clinical outcomes in Beijing Fuwai Hospital: A brief clinical review. ASAIO J 57: 414-420, 2011.
22. Ram Kumar RM, Boro A and Fuchs B: Involvement and clinical aspects of MicroRNA in osteosarcoma. Int J Mol Sci 17: 877, 2016.
23. Zhou B, Li L, Li Y, Sun H and Zeng C: Long noncoding RNA SNHG12 mediates doxorubicin resistance of osteosarcoma via miR-320a/MCL1 axis. Biomed Pharmacother 106: 850-857, 2018.
24. Huang S, Zhu X, Ke Y, Xiao D, Liang C, Chen J and Chang Y: LncRNA FTX inhibition restrains osteosarcoma proliferation and migration via modulating miR-320a/TXNRD1. Cancer Biol Ther 21: 379-387, 2020.
25. Lefebvre V, Angelozzi M and Haseeb A: SOX9 in cartilage development and disease. Curr Opin Cell Biol 61: 39-47, 2019.
26. Zhang XD, Wang YN, Feng XY, Yang JY, Ge YY and Kong WQ: Biological function of microRNA-30c/SOX9 in pediatric osteosarcoma cell growth and metastasis. Eur Rev Med Pharmacol Sci 22: 70-78, 2018.
27. Zhang W, Wei L, Sheng W, Kang B, Wang D and Zeng H: miR-1225-5p functions as a tumor suppressor in osteosarcoma by targeting Sox9. DNA Cell Biol 39: 78-91, 2020.
28. Ma L, Zhang L, Guo A, Liu LC, Yu F, Diao N, Xu C and Wang D: Overexpression of FER1L4 promotes the apoptosis and suppresses epithelial-mesenchymal transition and stemness markers via activating PI3K/AKT signaling pathway in osteosarcoma cells. Pathol Res Pract 215: 152412, 2019.
29. Qu H, Xue Y, Lian W, Wang C, He J, Fu Q, Zhong L, Lin N, Lai L, Ye Z and Wang Q: Melatonin inhibits osteosarcoma stem cells by suppressing SOX9-mediated signaling. Life Sci 207: 253-264, 2018.
30. Livak KJ and Schmittgen TD: Analysis of relative gene expression data using real-time quantitative PCR and the 2(-Delta Delta C(T)) method. Methods 25: 402-408, 2001.
31. Kai H, Koine T, Baba M and Okuyama T: Pharmacological effects of Daphne genkwa and Chinese medical prescription, 'Jyu-So-To'. Yakugaku Zasshi 124: 349-354, 2004 (In Japanese).
32. Chen Y, Guo J, Tang Y, Wu L, Tao W, Qian Y, Duan JA. Pharmacokinetic profile and metabolite identification of yuanhuapine, a bioactive component in Daphne genkwa by ultra-high performance liquid chromatography coupled with tandem mass spectrometry. J Pharm Biomed Anal 112: 60-69, 2015.
33. Huang YC, Lee PC, Wang JJ and Hsu YC: Anticancer effect and mechanism of hydroxygenkwanin in oral squamous cell carcinoma. Front Oncol 9: 911, 2019.
34. Villanueva F, Araya H, Briceño P, Varela N, Stevenson A, Jerez S, Tempio F, Chnaiderman J, Perez C, Villarroel M, et al: The cancer-related transcription factor RUNX2 modulates expression and secretion of the matricellular protein osteopontin in osteosarcoma cells to promote adhesion to endothelial pulmonary cells and lung metastasis. J Cell Physiol 234: 13659-13679, 2019.
35. Li C, Zhang S, Qiu T, Wang Y, Ricketts DM and Qi C: Upregulation of long non-coding RNA NNT-AS1 promotes osteosarcoma progression by inhibiting the tumor suppressive miR-320a. Cancer Biol Ther 20: 413-422, 2019.
36. De-Ugarte L, Balcells S, Guerri-Fernandez R, Grinberg D, Diez-Perez A, Nogues X and Garcia-Giralt N: Effect of the tumor suppressor miR-320a on viability and functionality of human osteosarcoma cell lines compared to primary osteoblasts. Appl Sci 10: 2852, 2020.
37. Lian F, Cui Y, Zhou C, Gao K and Wu L: Identification of a plasma four-microRNA panel as potential noninvasive biomarker for osteosarcoma. PLoS One 10: e0121499, 2015.
38. Li JH, Liu S, Zhou H, Qu LH and Yang JH: starBase v2.0: Decoding miRNA-ceRNA, miRNA-ncRNA and protein-RNA interaction networks from large-scale CLIP-Seq data. Nucleic Acids Res 42 (Database Issue): D92-D97, 2014.
39. Yu M, Bardia A, Wittner BS, Stott SL, Smas ME, Ting DT, Isakoff SJ, Ciciliano JC, Wells MN, Shah AM, et al: Circulating breast tumor cells exhibit dynamic changes in epithelial and mesenchymal composition. Science 339: 580-584, 2013.